JARO 19: 571–587 (2018)
DOI: 10.1007/s10162-018-0678-4

Research Article

JARO
Journal of the Association for Research in Otolaryngology

Psychophysical Tuning Curves as a Correlate of Electrode Position in Cochlear Implant Listeners

Lindsay DeVries[1] and Julie G. Arenberg[1]

[1]*Department of Speech and Hearing Sciences, University of Washington, 4131 15th Ave NE, Seattle, WA 98106, USA*

Received: 27 November 2017; Accepted: 23 May 2018; Online publication: 4 June 2018

ABSTRACT

Speech understanding abilities vary widely among cochlear implant (CI) listeners. A potential source of this variability is the electrode-neuron interface (ENI), which includes peripheral factors such as electrode position and integrity of remaining spiral ganglion neurons. Suboptimal positioning of the electrode array has been associated with poorer speech outcomes; however, postoperative computerized tomography (CT) scans are often not available to clinicians. CT-estimated electrode-to-modiolus distance (distance from the inner wall of the cochlea) has been shown to account for some variability in behavioral thresholds. However, psychophysical tuning curves (PTCs) may provide additional insight into site-specific variation in channel interaction. Thirteen unilaterally implanted adults with the Advanced Bionics HiRes90K device participated. Behavioral thresholds and PTCs were collected for all available electrodes with steered quadrupolar (sQP) configuration, using a modified threshold sweep procedure, used in Bierer et al. (Trends Hear 19:1–12, 2015). PTC bandwidths were quantified to characterize channel interaction across the electrode array, and tip shifts were assessed to identify possible contributions of neural dead regions. Broader PTC bandwidths were correlated with electrodes farther from the modiolus, but not correlated with sQP threshold, though a trend was observed. Both measures were affected by scalar location, and PTC tip shifts were observed for electrodes farther from the modiolus. sQP threshold was the only variable correlated with word recognition. These results suggest PTCs may be used as a site-specific measure of channel interaction that correlates with electrode position in some CI listeners.

Keywords: psychophysical tuning curves, cochlear implants, electrode position, imaging, psychophysics

Correspondence to: Lindsay DeVries · Department of Speech and Hearing Sciences · University of Washington · 4131 15th Ave NE, Seattle, WA 98106, USA. Telephone: 206-685-2194; email: lindsdev@uw.edu

INTRODUCTION

Cochlear implants (CIs) are neural prostheses that provide auditory input to people with severe-to-profound hearing loss. Outcomes are highly variable across listeners; performance on word and sentence tests ranges from 0 to 100 % (Koch et al. 2004; Won et al. 2007; Holden et al. 2013). A potential source of this high variability is the electrode-neuron interface (ENI), which includes peripheral components such as electrode position, bone and tissue growth, and the integrity of remaining spiral ganglion neurons (Bierer 2010; Pfingst et al. 2011; Long et al. 2014). Computational modeling, CT imaging, electrophysiological, and behavioral studies have demonstrated that behavioral thresholds are higher and spatial spread of excitation is broader for electrodes distant from target spiral ganglion neurons, or those that may be near degenerated neurons (Goldwyn et al. 2010; Long et al. 2014; Kalkman et al. 2014; DeVries et al. 2016). Broader spread of excitation increases channel interaction, or overlapping areas of neural activation, which may lead to poorer spectral resolution and decreased word understanding (e.g., Abbas et al. 2004; Hughes and Stille 2008; Jones et al. 2013).

Animal studies have demonstrated that long-term deafness results in smaller evoked potential responses and fewer surviving spiral ganglion neurons (Smith

and Simmons 1983; Hall 1990; Shepherd and Javel 1997; Ramekers et al. 2014). Human temporal bone studies have directly measured spiral ganglion survival rates in both non-CI and CI listeners, with rates ranging from 4 to 100 % survival (e.g., Hinojosa and Lindsay 1980; Linthicum et al. 1991; Khan et al. 2005). Others have studied potential indirect measures of neural health in CI listeners, such as behavioral thresholds (Long et al. 2014; Zhou and Pfingst 2016). Despite this, it is not currently possible to directly assess neural health in vivo in CI listeners.

Using CT imaging techniques, one can directly estimate a different component of the ENI—electrode position. CT imaging provides information including, but not limited to electrode-to-modiolus distance, scalar location, insertion angle, and wrapping factor (Verbist et al. 2005; Skinner et al. 2002; Teymouri et al. 2011; Holden et al. 2013). By quantifying this aspect of the ENI, deductive inferences may be made about neural status local to each electrode. Thus, disambiguating different aspects of the ENI may provide important information about the functional capacity of a given implant channel, which may have a direct effect on success with the device.

While CT imaging may offer insight into the ENI, this technique has notable disadvantages, such as high costs, exposing patients to radiation, no direct information about neural status, and limited availability. Therefore, an alternative method to measure electrode position is needed. A recent study in our laboratory compared aspects of electrode position to the electrically evoked compound action potential (ECAP); however, in that study, many participants did not have measureable ECAPs, or responses were noisy due to large stimulus artifact (DeVries et al. 2016). Therefore, evaluating a more reliable measure of channel interaction, such as the psychophysical tuning curve (PTC), is warranted.

Bierer and Faulkner (2010) demonstrated that broad PTCs were correlated with higher behavioral thresholds using focused stimulation, such that channels with higher thresholds had broader spatial tuning; these findings echoed those of Nelson et al. (2008) with bipolar stimulation. These studies suggest that focused PTCs may capture site-specific variations in spatial tuning. However, the use of PTCs has not been explored to estimate electrode-to-modiolus distance in CI listeners. Furthermore, PTCs have not been fully characterized across the electrode array, as most studies have examined a small subset of electrodes due to the lengthy testing time required with traditional psychophysical methods (e.g., Nelson et al. 2008, 2011). The present study used a faster method for obtaining focused PTCs based on a Békésy-like sweep procedure recently used for measuring focused thresholds in CI listeners (Bierer et al. 2015).

In broad terms, this study aims to assess (1) the viability of using PTCs as a site-specific measure of channel interaction, (2) if measures of electrode position allow for inferences about neural status, and (3) insight into the identification and assessment of poor ENIs.

Specifically, we quantify the relationship between PTC bandwidths, focused behavioral thresholds, and electrode-to-modiolus distances. We predict that channels with broader PTC bandwidths will have (1) larger electrode-to-modiolus distances, (2) scalar locations outside of scala tympani, and (3) higher focused thresholds. Other comparisons between focused behavioral thresholds, electrode-to-modiolus distance, scalar location, PTC tip location, and word recognition were made.

These findings may help advance understanding of the complexities of the ENI and how site-specific measures of channel interaction relate to word recognition.

METHODS

Subjects

Thirteen adult subjects who were unilaterally implanted after 2001 with Advanced Bionics HiRes90k devices participated (Table 1). Subjects were at least 21 years of age ($M = 62.8$, SD = 15.3), and eight were males. Two subjects were pre-lingually deafened (diagnosed with severe to profound hearing loss before the age of 4), one was peri-lingually deafened (diagnosed with severe to profound hearing loss at age 4), and the remaining ten were post-lingually deafened. Two subjects were deafened in childhood (S54, age 7, and S46, age 14), but are still considered with the post-lingually deafened subjects as they learned language before they were diagnosed with a severe-to-profound hearing loss. All subjects were fluent English speakers. Each participant provided written consent, and the experiments were conducted in accordance with guidelines set by the University of Washington Human Subjects Division.

CT Imaging

CT scans were performed at the University of Washington Medical Center within the last 3 years. CT scans were analyzed at Washington University in St. Louis, MO. Briefly, ANALYZE software was used to create 3-dimensional image volumes by combining information from each subject's postoperative scan and a single body donor cochlea (Fig. 1; for details, see Skinner et al. 2002; for verification of the method, see Teymouri et al. 2011). Preoperative CT scans were not available for the subjects participating in the

TABLE 1

The demographic information for all 13 subjects including ear implanted, chronological age, age diagnosed with a profound hearing loss, age at implantation, duration of deafness, etiology (if known), electrode array type and electrode spacing, and clinical CNC word score

ID	*Ear*	*Age*	*Age at profound HL*	*Age implanted*	*Duration of deafness (years)*	*Etiology*	*Electrode array/spacing (mm)*	*CNC word score (%)*
S22	R	77	55	66	11	Suspected genetic	1-J Helix/0.85	50
S29	L	86	47	77	30	Noise	HiFocus 1 J/1.1	76
S40	L	55	4	50	46	EVA	HiFocus 1 J/1.1	20
S42	R	67	50	50	0	Idiopathic	HiFocus 1 J Pos./0.9	93
S43	R	71	50	67	17	Noise	Mid-Scala/0.85	78
S46	R	66	14	62	48	Unknown	HiFocus 1 J/1.1	30
S47	R	68	28	37	9	Unknown	Mid-Scala/0.85	83
S49	R	44	1.5	43	41.5	Suspected genetic	Mid-Scala/0.85	30
S53	R	54	1	44	43	Meningitis	1-J Helix/0.85	84
S54	L	26	7	23	16	Suspected EVA	Mid-Scala/0.85	72
S55	R	63	41	49	8	Suspected genetic	HiFocus 1 J/1.1	92
S56	L	72	30	58	28	Idiopathic	HiFocus 1 J Pos./0.9	76
S57	R	67	63	65	2	Idiopathic	Mid-Scala/0.85	62

present study; therefore, a scan of the non-implanted ear was used to identify structural anatomy, and this image was co-registered with the image of the implanted ear. Micro CT and orthogonal-plane fluorescence optical sectioning (OPFOS) images from a donor cochlea were used to locate and visualize the non-bony structures. The two CT-estimated metrics used in this study were electrode-to-modiolus distance and scalar location. Electrode-to-modiolus distance refers to the lateral distance (mm) of an electrode from the medial wall of the cochlea. Scalar location denotes the positioning of an electrode in the fluid-filled cochlear compartments: scala tympani (ST), intermediate, and scala vestibuli (SV). Intermediate refers to those electrodes that could not be clearly determined to be in ST or SV.

Electrical Stimulation

All stimuli were presented using the Bionic Ear Data Collection System version 1.18.315 (Advanced Bionics, Valencia, CA). For behavioral testing, a custom Matlab (Mathworks, Inc. Natick, MA) script controlled the BEDCS software. Two types of electrode configurations were used in this study: monopolar (MP) and steered quadrupolar (sQP). MP stimulation consists of an active intracochlear electrode and a return extracochlear electrode; the large distance between the source/sink yields a broad electrical field. sQP stimulation was used in the present study as it has been found to be equivalent to partial tripolar in another study, in which many of the same subjects participated (Bierer et al. 2015). sQP stimulation consists of four intracochlear electrodes: the two middle electrodes serve as active electrodes, and the two outer electrodes serve as return electrodes for a fraction of the active current (an extra cochlear electrode carries the remainder of the return current). Current is steered between the two middle electrodes according to the fraction, α with a value of one steers' current to the basal electrode and 0 to the apical electrode. By convention, channel number is defined as the basal active electrode when $\alpha = 1$. In the present study, this convention was maintained for electrodes 3 to 15. For electrode 2, however, it was necessary to use the same set of electrodes as channel 3 (the most apical channel possible with the 4-electrode sQP configuration) in conjunction with an α value of 0 to center the current on electrode 2. This arrangement is referred to as "channel 2," even though electrode 2 is the apical active electrode. For current focusing, the outer two electrodes in the sQP configuration receive a fraction of the return current according to σ (Landsberger and Srinivasan 2009; Srinivasan et al. 2010; Bierer et al. 2015). As with the commonly used partial tripolar configuration, higher σ results in a narrower electrical field than MP stimulation (Litvak et al. 2007). A value of $\sigma = 0.5$ was used in the present study for masker stimulation to retain sufficiently focused stimulation while avoiding unreasonably high current limits and side-lobe activation. For the shorter duration probe stimulation, an σ value of 0 (monopolar) was used to ensure the probe stimulus was salient to the listener. MP stimulation was used for probe stimuli, rather than sQP stimulation, because the high current requirements to achieve most comfortable level (MCL) for a very brief pulse train were often unobtainable within the compliance limits of the device with sQP; further, some subjects could not

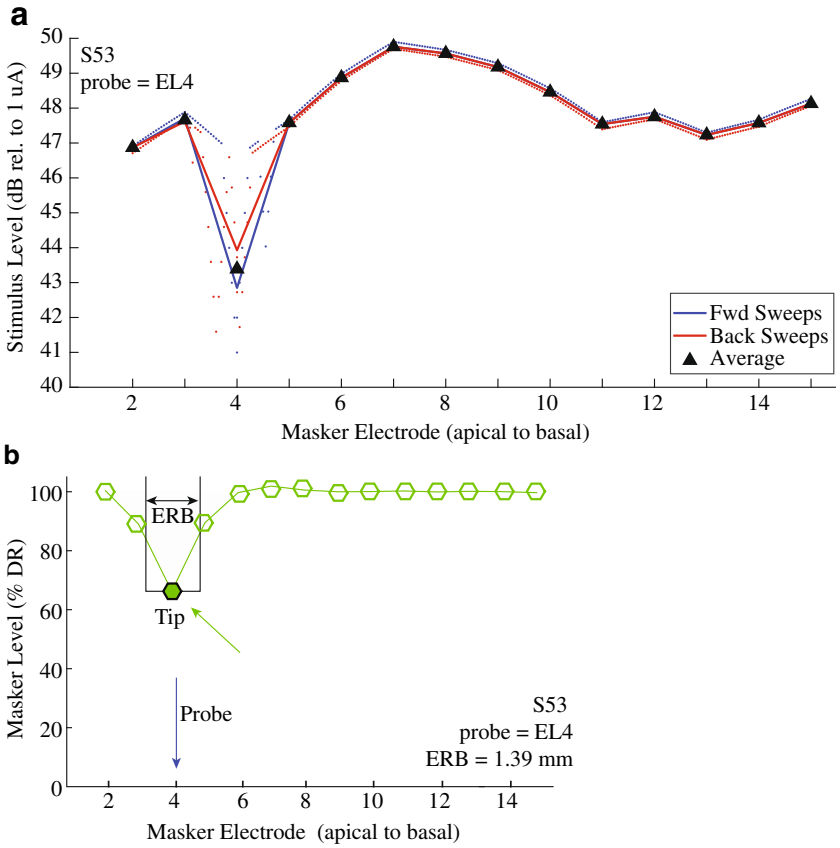

FIG. 1. **a** Example of one forward (blue) and one reverse (red) sweep for S53, probe 4. The *x*-axis is masker electrode (apical to basal), and the *y*-axis is stimulus level (dB rel. to 1 μA). The black triangles represent the mean masker level for each of the cardinal electrodes. **b** Example PTC for S53, probe 4. The *x*-axis is masker electrode (apical to basal), and the *y*-axis is masker level (percent dynamic range). The PTC ERB_{DR} is labeled (black rectangle), and the PTC ERB_{DR} value is marked inside the plot. The PTC tip (filled green circle) and probe electrode (blue arrow) are also labeled

perceive the probe stimulus using the more focused sQP stimulation. A fixed probe level measured in percent dynamic range was used to facilitate direct comparisons of PTCs across electrodes and subjects (McKay 2012).

Most Comfortable Listening Levels

MCLs were measured for use in the PTC procedure, described below. MCLs for masker and probe stimuli were determined using the Advanced Bionics clinical loudness scale (Advanced Bionics, Valencia, CA). To determine MCL, current level was increased manually until subjects reported a loudness rating of "6," or "most comfortable." The level was changed in 2 dB steps until a loudness rating of 4 was reached; thereafter the level was changed in 0.5 or 0.1 dB steps, depending on subject response. Device compliance limits were not reached for any subject. MCLs served as the maximum stimulus level for all psychophysical procedures.

Single-Channel Behavioral Thresholds

Single-channel thresholds were measured for electrodes 2–15 using the sweep threshold procedure (Bierer et al. 2015). Stimuli were biphasic, cathodic-leading pulses trains (102 μs/ph, 0-μs interphase gap, 200.4 ms duration, 997.9 pulses per second) using sQP stimulation with $\sigma = 0.9$; highly focused thresholds were measured to capture local variability for later comparison with PTC measures. Pulse trains were presented starting at 6 dB below the MCL, with α-value increasing from 0 to 1 in 0.1 steps from electrode 2–15 for a forward sweep (apical to basal), and from 15 to 2 (basal to apical), for a backward sweep (based on Sęk et al. 2005; for details, see Bierer et al. 2015). A forward and backward sweeps were run for each set of stimuli and averaged to estimate thresholds. Device compliance limits were not reached for any subject during threshold measurement. Sweep thresholds served as the minimum stimulus levels for all psychophysical procedures.

Sweep Psychophysical Tuning Curves

Single-channel behavioral thresholds were measured for masker and probe stimuli using sQP stimulation and the threshold sweep procedure (Bierer et al. 2015). Stimuli were biphasic, cathodic-leading pulse trains (102 μs/ph, 0-μs interphase gap, 997.9 pulses per second), presented to electrodes 2–15 (apical to basal), for both masker (200.4 ms duration) and probe (20 ms duration) stimuli. Masker stimuli were presented with sQP stimulation using an $\sigma = 0.5$; probe stimuli used $\sigma = 0$. These thresholds determined the lower limit of stimulation, and the MCLs determined the upper limit.

PTCs were obtained for all available electrodes within a forward-masking paradigm using a modified threshold sweep procedure (Fig. 1a; Bierer et al. 2015). This procedure is similar to the sweep threshold procedure (see single-channel behavioral thresholds section), though in this case the masker was swept across the electrode array, varying in level, while the probe remained fixed in level and location. Each PTC sweep took approximately 6 min, with a total of 24 min per electrode for a complete PTC. Probe stimuli were presented at 30 % probe dynamic range when possible; for some subjects, the level was increased to 40–50 % dynamic range due to some subject's inability to do the task with the probe at a softer level. Probe levels were set as a percentage of the probe dynamic range to ensure that the stimuli were consistently soft and equally loud across all probe electrodes (McKay 2012). Masker levels were normalized to the percentage of the masker dynamic range, which reduces variability and allows for ease of comparison across all probe electrodes and subjects.

The listener was presented with a box on the computer screen and instructed to hold down the space bar when they heard the target sound (probe) and release the space bar when they no longer heard it. This procedure was repeated until all available electrodes served as probes. Two subjects, S40 and S49 had difficulty with the sweep PTC procedure; they were unable to hear the probe in the presence of the masker, even at higher levels and at longer masker-probe intervals. In those cases, a two-interval, two-alternative, forced choice (2IFC) procedure, identical to that used by Bierer and Faulkner (2010) was used for all electrodes to explore the central hypothesis. A recent study by Bierer et al. (2015) did not find any systematic differences between 2IFC thresholds and the threshold sweep procedure, which allows for significantly faster collection of psychophysical data.

PTC Quantification

PTCs were characterized as a function of masker level, normalized to the masker-alone dynamic range. The equivalent rectangular bandwidth (ERB_{DR}) was used to quantify the spatial extent of masker-probe interaction by equating the PTC to a rectangular function of equivalent minimum masker level (Fig. 1b). It was calculated by dividing the area above the PTC by the minimum masker level (PTC tip). This is a commonly used method in psychoacoustics, which avoids selection of a fixed masker level from which a PTC bandwidth is often derived. PTCs with probes near the end of the electrode array (typically electrodes 2 and 15) were not fully characterized on one side due to the lack of electrodes to use as maskers. Partial tuning curves were defined as those for which the tip of the PTC was determined to be at the end of the electrode array. Under the assumption that neural excitation would extend to neurons beyond the array, partial tuning curves were completed by mirroring the masker levels from the measured data on the side with a full complement of masker electrodes.

PTC tip shifts were quantified to examine the relationship between suspected areas of poor neural health and electrode position. For each subject, two runs of PTC sweeps were collected. One run consists of forward and backward sweeps. The difference between PTC sets was calculated and averaged to assess within-subject variability between sweep sets. This resulted in an individual criterion cut-off for what was considered a tip shift. For example, if there was a 15 % mean difference between PTC sets, a greater than 15 % difference between the masker level at the probe and the tip (the minimum masker level) was considered to be a tip shift. Table 2 shows

TABLE 2

Individual mean difference (percent masker dynamic range) and standard deviation between two sets of PTC sweeps

ID	*Mean Diff. (%DR)*	*SD (±)*	*No. of tip shifts*
S22	12.3	0.09	5
S29	12.5	0.12	4
S40	11.5	.08	4
S42	19.5	0.25	4
S43	18.1	0.15	3
S46	17.9	0.16	4
S47	12.6	0.09	1
S49	11.9	.08	4
S53	14.8	0.18	2
S54	13.7	0.11	2
S55	8.9	0.08	4
S56	9.3	0.08	1
S57	13.5	0.11	1

For S40 and S49, the values were calculated by comparing each run from the 2IFC procedure. The mean differences are used as criterion for whether a PTC tip shift occurred

the tip shift criterion used, standard deviation between PTC sets, and number of tip shifts for each subject. There were 39 tip shifts out of the 182 PTCs. There were eight PTCs with tips shifted by more than one electrode. There were 19 apical and 20 basal tip shifts in this dataset. The tip shifts were collapsed across electrodes and are reported as "tip shift" or "no tip shift" and analyzed as a binary variable.

Word Recognition

Scores on a word recognition task were obtained to evaluate clinical performance in the context of sQP threshold, electrode-to-modiolus distance, and PTC ERB_{DR}. Performance on the consonant-nucleus-consonant (CNC) words was obtained from each subject's clinical audiologist. Per audiologist report, the CNC words were presented at 60 dB-SPL in the sound field using the subject's everyday speech processor program. For subjects S46 and S49, the only scores available from the audiologist were in the bimodal condition; therefore, they were tested in the laboratory in the CI-only condition at 60 dB-SPL in the sound field using the subject's everyday speech processor program. All scores were from within the last 2 years and are reported in Table 1.

Statistical Analysis

SPSS statistical software was used to perform linear mixed effect analyses for between-subjects comparisons (IBM Corp. Released 2015. IBM SPSS Statistics for Windows). The first analysis assessed whether PTC ERB_{DR}s measured with the 2IFC procedure (used for S40 and S49) significantly differed from those subjects who used the modified threshold sweep procedure. This analysis showed no significant effect of psychophysical task on PTC ERB_{DR}s ($F(20.3) = .18$, $P = .68$); therefore PTC ERB_{DR}s from both tasks were compiled in all following statistical models.

The first model included sQP threshold as the dependent variable, electrode-to-modiolus distance as the independent variable of interest, and duration of deafness as a covariate. The second analysis included PTC ERB_{DR} as the dependent variable, with sQP threshold, and electrode-to-modiolus distance as fixed factors, and duration of deafness as a covariate. Duration of deafness was added as a continuous covariate in these models due to the presence of two pre- (S49, S53) and one peri-lingually (S40) deafened subject in this dataset; these three subjects have similar durations of deafness (41.5, 43, and 46 years, respectively). Additional linear mixed effect analyses were conducted to evaluate the effects of scalar location (dependent ordinal variable) on sQP threshold, electrode-to-modiolus distance, and PTC ERB_{DR}. For all mixed effects models, electrode was added as the repeated factor, and subjects were entered as a random factor, so that each subject had their own intercept for the effects of interest (Baayen et al. 2008). A Bonferroni correction was applied to all multiple comparisons and is noted where appropriate; all *p*-values reported from this procedure are adjusted for a significance level of $\alpha = .05$.

A generalized estimating equation (GEE) procedure was performed to evaluate the presence of a tip shift (dependent binary variable) on sQP threshold, electrode-to-modiolus distance, and PTC ERB_{DR} (independent continuous variables). The GEE procedure extends the generalized linear model to allow for a repeated measures analysis on a binary dependent variable (IBM Corp. Released 2015. IBM SPSS Statistics for Windows); reported results are from a Wald's test.

A multiple linear regression analysis was performed to evaluate the relationship between clinical CNC scores and mean electrode-to-modiolus distance, mean sQP threshold, and mean PTC ERB_{DR}.

RESULTS

Electrode-to-Modiolus Distance Using CT Imaging

Figure 2 highlights the variability in electrode array positioning observed in 3D cochlear reconstructions for all subjects, arranged by electrode array type. In general, the electrode trajectories in Fig. 2 are consistent with the designs of the four types of arrays, which partially determine how far the electrodes are from the modiolus, and thus how close they are to target auditory neurons. The 1 J electrode array (S29, S40, S46, and S55) has a lateral design, whereas the 1-J Helix (S22, S53) is pre-curved to achieve a more medial position. The 1 J with positioner (S42, S56), by design, pushes the electrode array even more medially. The Mid-Scala array (S43, S49, S47, S54, S57) is pre-curved and designed for mid-scalar placement to protect cochlear structures.

Focused Behavioral Thresholds and Electrode-to-Modiolus Distance

Figure 3a shows electrode-to-modiolus distance (left ordinate) and sQP threshold (right ordinate) profiles for each subject. Scalar location is indicated by symbol (see legend). sQP thresholds ranged from 28.8–55.7 dB rel. to 1 μA ($M = 45.67$ dB rel. to 1 μA, SD = 6.12) across all subjects and electrodes (Table 3). Electrode-to-modiolus distance, or the lateral distance in millimeters from the modiolus, ranged from 0.18 to 2.2 mm ($M = 1.06$ mm, SD = .52; see Table 3). Figure 3b illustrates the relationship between sQP

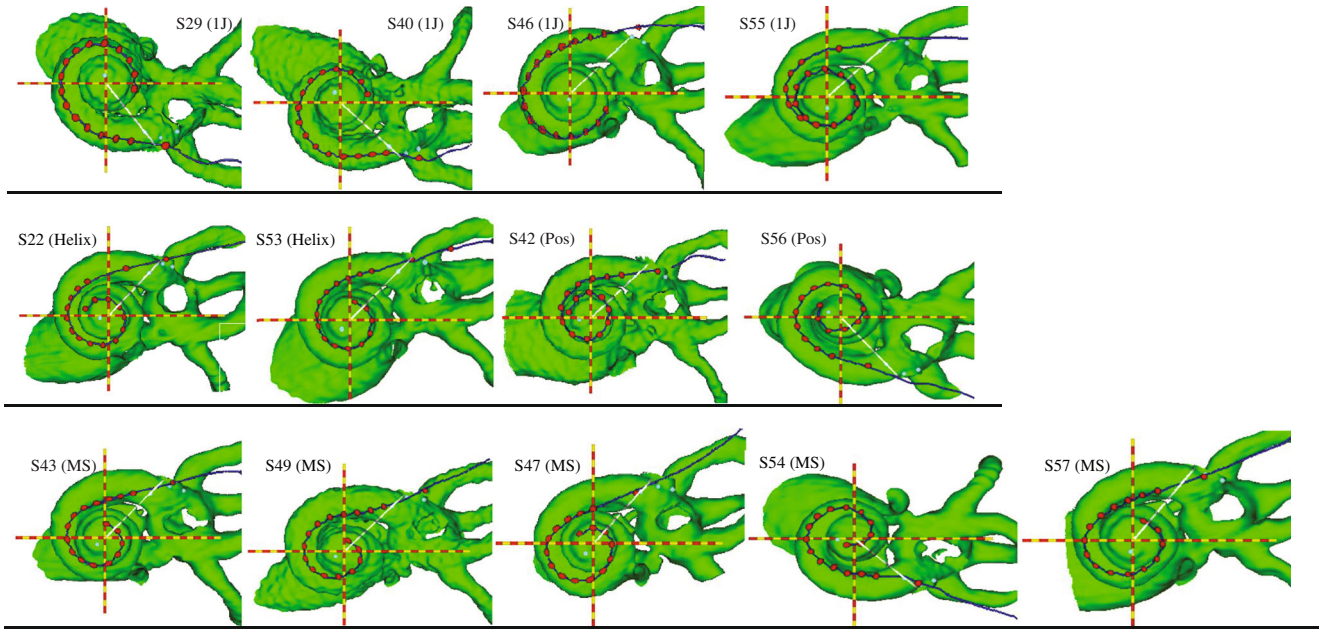

FIG. 2. CT view of cochlea and electrode array along the midmodiolar axis (red and yellow dashed lines), for all subjects, organized by electrode array type. The evenly spaced red dots represent electrodes; the outermost dot represents the insertion depth marker. The white line represents the 0 ° reference point from which insertion depth is measured, extending from the midmodiolar axis. Row 1: 1 J; row 2: 1-J Helix and 1 J with positioner; row 2: Mid-Scala electrode array

threshold and electrode-to-modiolus distance, with individual subject data distinguished by color and shape; the line of best fit for all subjects is plotted (solid black). Figure 4c shows the line of best fit for individual subjects, as well as the group line of best fit (solid black). Consistent with previous studies (Long et al. 2014; Cohen et al. 2003), a strong association between sQP thresholds and electrode-to-modiolus distance was observed. Results from the linear mixed effect analysis show a significant relationship between electrode-to-modiolus distance and sQP threshold ($F(1,170.5) = 57.33$ $P < .001$); in other words, across subjects, electrodes with higher behavioral thresholds tended to be farther from the modiolus. It is worth noting that for the six subjects where this relationship was observed (S42, S43, S47, S49, S53, S57), four have the Mid-Scala electrode array; the other two subjects have 1 J with positioner and a 1-J Helix array. For subjects with the 1-J array (S29, S40, S46, S55), which tends to sit laterally to the modiolus, electrode-to-modiolus distance did not correlate with sQP threshold, likely due to low variability in electrode position in this data set. Due to the small sample size for each electrode array, statistical differences between array types cannot be further examined.

While duration of deafness significantly contributed to this relationship ($F(11.6) = 15.4$ $P < .001$), duration of deafness did not dictate whether a correlation between sQP threshold and electrode-to-modiolus distance existed. Those subjects with longer durations of deafness tended to have higher thresholds overall, but this did not preclude a significant, positive correlation with electrode distance; the line of best fit was simply shifted up the *y*-axis for these subjects.

Psychophysical Tuning Curve Characteristics

There was wide variability observed in the PTCs within and across subjects. Across subjects, PTC ERB_{DR}s ranged from 0.70 to 10.40 mm, with a mean of 3.62 mm (SD = 2.01; Table 3). There was a total of 39 tip shifts out of 182 PTCs; S22 had the greatest number of tip shifts at five (see Table 2). There was no apparent effect of apical or basal-ward tip shifts in the data.

Figure 4 shows all 14 PTCs across the electrode array for three example subjects S56 (a), S57 (b), and S53(c). PTCs are plotted as masker level (% dynamic range) as a function of masker electrode (apical to basal). The mean ERB_{DR} for these subjects is marked on each panel. There was a high degree of overlap, or presumed channel interaction, between PTCs within a given subject. This is particularly evident for S56 (Fig. 4a), where most PTCs are overlapping, and some PTC tips (such as electrode 3) are shifted quite far basally, and some apically (electrode 5). S57 (Fig. 4b) had quite deep PTCs, with few tip shifts; however, a high degree of PTC overlap is observed across the electrode array. S53 (Fig. 4c) had shallower PTCs apically, and deeper PTCs basally; there are more

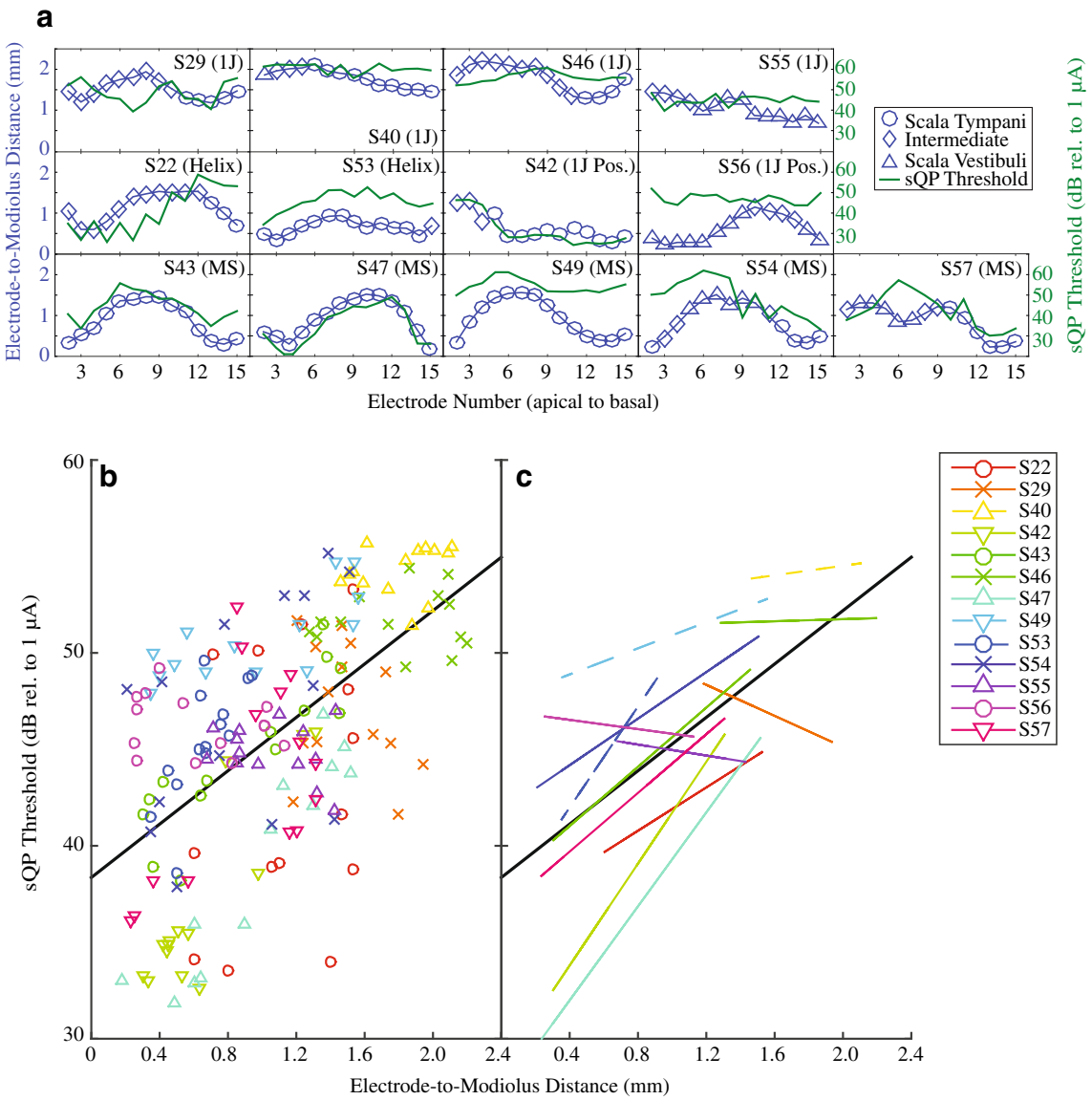

FIG. 3. **a** sQP threshold in dB rel. to 1 µA (green line) and electrode-to-modiolus distance in mm (blue line) for all subjects, organized by electrode array type. Scalar information is represented by symbols along the electrode-to-modiolus distance line: ST (circles), Intermediate (diamonds), and SV (triangles). **b** Scatter plot comparing electrode-to-modiolus distance with sQP threshold for individual subjects (distinguished by color) and the line of best fit for all subjects (solid black line). **c** The line of best fit for individual subjects for the data in panel B (lines distinguished by color), and for all subjects (solid black line)

easily observable PTC tips and less channel interaction overall. Interestingly, though the PTC characteristics of these example subjects differ, their clinical performance is very similar (Table 1).

Comparisons between Focused Thresholds, Electrode-to-Modiolus Distances, and Tuning Curve Bandwidths

Scatterplots of PTC ERB_{DR}s and electrode-to-modiolus distance (Fig. 5a), and sQP thresholds (Fig. 5c) are shown for all subjects, with individual data distinguished by color and shape. Figure 5b, d show the lines of best fit for individual subjects and the group (solid black line). Table 4 shows results for within-subject correlations for these comparisons. Results from the linear mixed effect analysis show PTC ERB_{DR}s are correlated with electrode-to-modiolus distance ($F(1,163.87) = 9.30$, $P = .003$). Although there was a trend toward higher sQP thresholds for broader PTC ERB_{DR}s, there was no statistically significant effect ($F(1,177.83) = 3.14$ $P = .08$). There was no effect of duration of deafness ($F(1,13.96) = .02$, $P = .89$). These results indicate that PTC ERB_{DR}s are broader for electrodes farther from the modiolus, but that PTC

TABLE 3

Means and standard deviations for electrode-to-modiolus distance, sQP threshold, and tuning equivalent rectangular bandwidth (ERB_{DR}); data shown are for electrodes 2–15

ID	*EMD (mm) mean (SD)*	*Focused thres. (dB) mean (SD)*	*Tuning ERB_{DR} (mm) mean (SD)*	*Threshold-distance RMS error*	*%DR for PTCs*
S22	1.12 *(.37)*	42.72 *(6.92)*	2.14 *(1.14)*	6.22	30
S29	1.52 *(.23)*	47.15 *(3.32)*	3.70 *(1.37)*	3.31	40
S40	1.79 *(.22)*	54.27 *(1.30)*	5.40 *(2.40)*	1.32	50 (2IFC)
S42	.64 *(.33)*	36.96 *(4.80)*	3.07 *(1.73)*	2.3	30
S43	.84 *(.44)*	44.69 *(3.95)*	3.09 *(1.48)*	1.9	40
S46	1.80 *(.34)*	50.67 *(1.58)*	5.51 *(2.23)*	1.59	30
S47	.87 *(.46)*	38.39 *(5.91)*	2.61 *(.76)*	2.08	30
S49	.94 *(.47)*	50.70 *(2.15)*	2.85 *(1.02)*	1.49	40 (2IFC)
S53	.66 *(.17)*	45.41 *(3.01)*	2.30 *(.96)*	2.09	30
S54	.89 *(.46)*	47.14 *(5.77)*	3.16 *(1.43)*	5.27	50
S55	1.06 *(.26)*	44.88 *(1.47)*	5.81 *(1.74)*	1.48	40
S56	.62 *(.33)*	46.26 *(1.53)*	4.51 *(2.62)*	1.53	30
S57	.90 *(.39)*	43.39 *(4.32)*	2.89 *(1.27)*	4.58	30
Summary	1.06 *(.52)*	45.68 *(6.13)*	3.62 *(2.01)*	N/A	N/A

Threshold-distance RMS error, number of tip shifts, and %DR used for PTCs are also listed. The summary line indicates means and standard deviations across subjects

ERB_{DR}s were not a reliable correlate of focused behavioral thresholds in these subjects.

Scalar Location

CT-estimated scalar location was assessed for all subjects and electrodes. Of 182 electrodes, 54.4 % were in ST, the target scalar location during surgical implantation. Most of the other electrodes were estimated to be in the intermediate position (28 %), with the remaining electrodes in the SV (17.6 %). Figure 6 presents box plots of the distribution of scalar location for sQP threshold (a), electrode-to-modiolus distance (b), and PTC ERB_{DR} (c). Results from the linear mixed effect analysis show a main effect of scalar location for sQP threshold ($F(1.174.7) = 7.59$, $P = .001$), electrode-to-modiolus distance ($F(1.177.31) = 18.93$, $P < .0001$), and PTC ERB_{DR} ($F(1,170.09) = 7.0$, $P < .01$).

After Bonferroni adjustment, results show that sQP thresholds were higher for electrodes in SV as compared to ST ($P < .0001$) and as compared to electrodes in the intermediate position ($P = .05$). There were no significant differences in sQP threshold between intermediate electrodes and those in ST ($P = .11$). As expected, electrodes located in either SV ($P = .003$) or the intermediate position ($P < .001$) had greater electrode-to-modiolus distances as compared to ST; there were no significant differences between electrodes in SV and the intermediate position ($P = .58$). As sQP threshold and electrode-to-modiolus distance was shown to be correlated in this study and others (Long et al. 2014; DeVries et al. 2016), these results indicate that for electrodes in SV, high sQP thresholds may be primarily driven by electrode position. PTC ERB_{DR}s were significantly broader for electrodes in SV ($P < .01$) as compared to ST but did not reach statistical significance when compared to electrodes in the intermediate position ($P = .06$). There were no significant differences in PTC ERB_{DR}s between intermediate electrodes and those in ST ($P = .19$).

It is important to interpret these analyses with caution. While the linear mixed effect analysis accounts for uneven sample sizes, the boxplots show that the distributions of the variables of interest tend to overlap substantially in many cases (particularly with sQP threshold). This may signify that the statistically significant effects observed are small in magnitude.

Effect of PTC Tip Shifts

Results from the GEE procedure (see "Statistical Analysis") show no effect of tip shift for sQP threshold ($\chi^2 = 2.33$, $P = .13$; Fig. 7a) or PTC ERB_{DR} ($\chi^2 = .50$, $P = .48$; Fig. 7a). Interestingly, there was a significant effect of tip shift for electrode-to-modiolus distance ($\chi^2 = 7.35$, $P = .007$; Fig. 7b), wherein electrodes with PTC tip shifts were likely to be positioned more lateral to the modiolus.

Further analyses were conducted to ascertain whether the number of within-subject tip shifts were correlated with high sQP thresholds not predicted by electrode-to-modiolus distance (quantified as greater than + 1 SD above the mean). In other words, we examined whether high sQP thresholds not accounted for by electrode position were correlated with more tip shifts, and thus possibly indicative of poor neural health. However, a linear regression showed that tip shifts were not

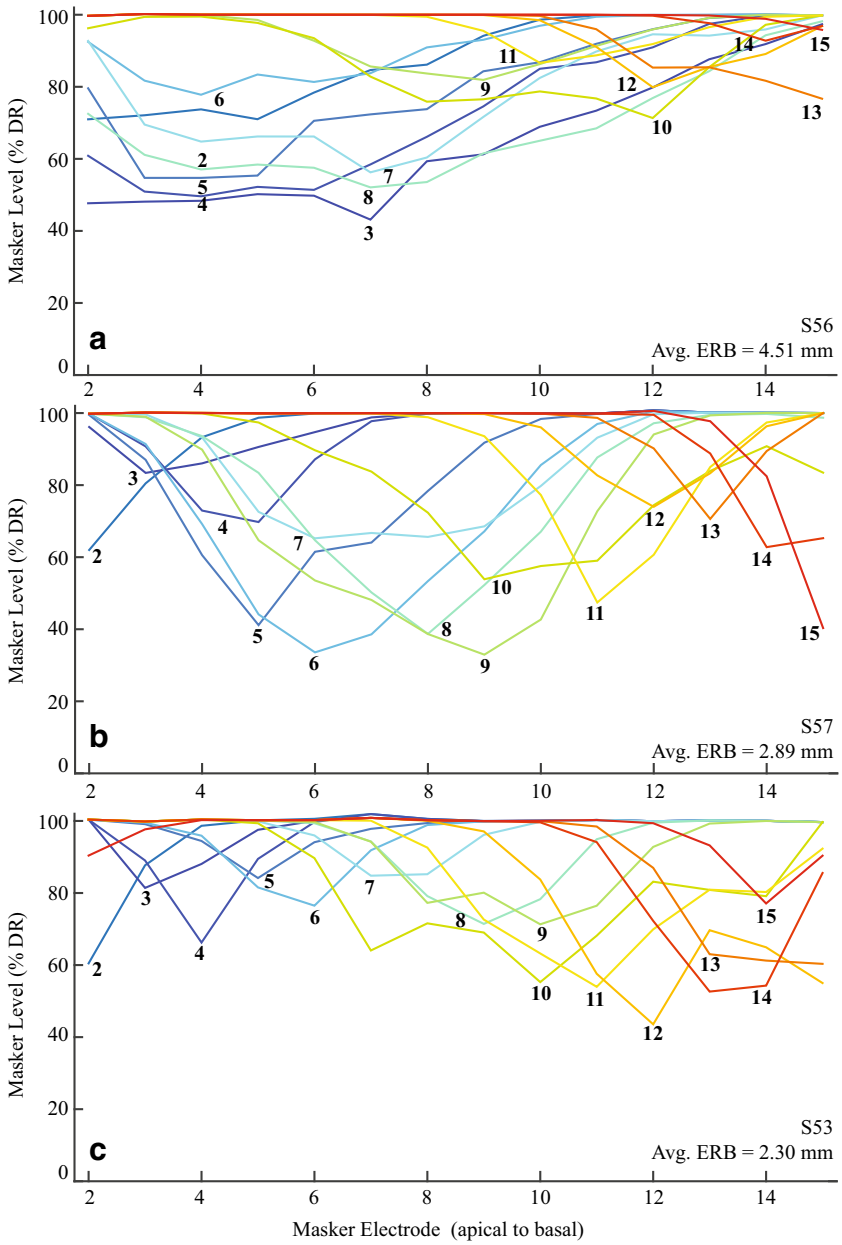

FIG. 4. PTCs across the electrode array for three example subjects (S56, S53, and S57). The *x*-axis denotes the masker electrode (apical to basal). The *y*-axis represents the masker level in percent dynamic range. The numbered lines inside the plot are probe electrodes, labeled at the tip of the PTC. The mean PTC ERB_{DR} in mm is marked inside each plot

correlated with sQP thresholds + 1 SD from the best-fit line ($F(1,11) = 1.68$, $P = .22$).

Word Recognition

Figure 8 shows mean performance on the CNC word test (% correct) in relation to mean sQP threshold (a), mean electrode-to-modiolus distance (b), and mean PTC ERB_{DR} (c). This set of predictors accounted for a significant amount of variance in CNC word scores ($R^2 = .72$, $F(3,9) = 7.56$, $P = .008$, $R^2_{adjusted} = .62$). The model shows no significant effect of mean PTC ERB_{DR} ($T_{19} = 1.65$, $R = -.26$, $P = .13$) or mean electrode-to-modiolus distance ($T_{19} = -1.76$, $R = -.66$, $P = .11$). sQP thresholds had a unique positive effect on CNC word scores ($T_{19} = -2.86$, $R = -.76$, $P = .02$), wherein subjects with higher mean sQP thresholds across the array tended to have lower CNC word scores.

DISCUSSION

The present study assessed the relationship between PTC ERB_{DR}s, sQP behavioral thresholds and

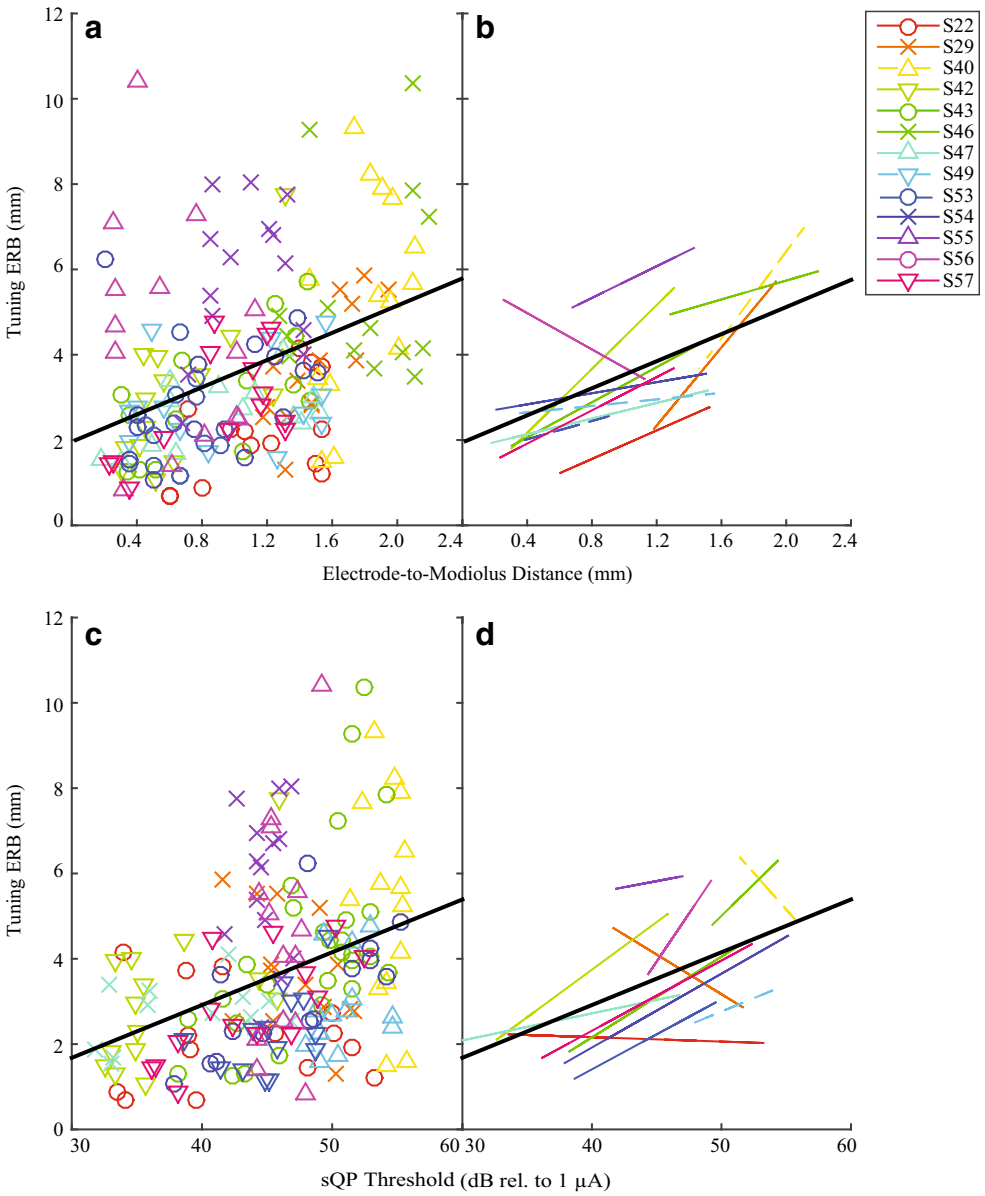

FIG. 5. Comparisons between sQP threshold, electrode position, and PTC ERB_{DR}s for individual subjects. **a** Electrode-to-modiolus distance and PTC ERB_{DR} individual data and group best fit line. **b** Electrode-to-modiolus distance and PTC individual and group best-fit lines **c** sQP threshold and PTC ERB_{DR} individual data and group best fit line. D: sQP threshold and PTC ERB_{DR} individual and group best-fit lines

CT-estimated electrode position. Results support the hypothesis that electrodes farther from the modiolus tend to have higher behavioral thresholds, broader PTC ERB_{DR}s, are translocated to SV, and a higher number of PTC tip shifts across the electrode array. There was no relationship observed between sQP thresholds and PTC ERB_{DR}s or tip shifts. Mean sQP thresholds were correlated with word recognition, whereas mean PTC ERB_{DR}s and mean electrode-to-modiolus distances were not, indicating that sQP thresholds may capture an additional aspect of the electrode-neuron interface important for speech perception.

Focused Single-Channel Behavioral Thresholds and Electrode-to-Modiolus Distance

Consistent with other studies, sQP thresholds were correlated with electrode-to-modiolus distance, such that electrodes with higher thresholds had larger electrode-to-modiolus distances (Cohen et al. 2001; Cohen 2009; Long et al. 2014; DeVries et al. 2016). As

TABLE 4

Individual Pearson's *r* and *p* values (* indicates statistical significance) for the correlations between: PTC ERB_{DR}s and sQP thresholds (dB rel. to 1 μA), in the left two columns, labeled threshold-ERB_{DR}, and between PTC ERB_{DR}s and electrode-to-modiolus distance (EMD; mm) in the right two columns, labeled as EMD-ERB_{DR}

ID	*r (threshold-ERB_{DR})*	*p (threshold-ERB_{DR})*	*r (EMD-ERB_{DR})*	*p (EMD-ERB_{DR})*
S22	−.06	.83	.53	.05*
S29	−.45	.11	.81	.0004*
S40	−.18	.53	.47	.09
S42	.62	.02*	.70	.006*
S43	.53	.053	.66	.01*
S46	.20	.48	.17	.56
S47	.49	.08	.55	.04*
S49	.26	.36	.18	.55
S53	.51	.06	.19	.51
S54	.70	.006*	.21	.48
S55	.05	.87	.28	.34
S56	.26	.36	−.27	.35
S57	.69	.006*	.60	.02*

duration of deafness increased, sQP thresholds tended to be higher, but this did not preclude a significant relationship with electrode-to-modiolus distance in some subjects. These findings are supported by histological data (Kawano et al. 1998), computational modeling (Briaire and Frijns 2006; Frijns et al. 1995, 1996; Goldwyn et al. 2010), and EABR thresholds in animals (Shepherd et al. 1993).

Figure 3b, c demonstrates that electrode-to-modiolus distance does not account for all the variability in sQP thresholds. It may be presumed that sQP thresholds not predicted by electrode-to-modiolus distance reflect areas with poor neural survival, though bone and tissue growth and tissue impedance may affect this relationship as well.

PTC Bandwidths, Electrode-to-Modiolus Distance, and Focused Single-Channel Behavioral Thresholds

Electrodes with broader PTC ERB_{DR}s were correlated with electrodes located farther from the modiolus, consistent with previous studies that used electrophysiological (Brown et al. 1990; Cohen et al. 2003; Hughes and Abbas 2006; DeVries et al. 2016) and modeling techniques (Briaire and Frijns 2006). PTC ERB_{DR}s were not correlated with sQP thresholds, though results trended toward significance in the expected direction. This result is consistent with a recent study in our laboratory that used the electrically evoked compound action potential (DeVries et al. 2016).

sQP thresholds likely capture the effects of electrode-to-modiolus distance and other factors such as neural status, which may explain the lack of relationship between sQP thresholds and PTC ERB_{DR}s. It is also possible that ERB_{DR}s are unable to capture this relationship. Other studies have used slopes or fixed widths to quantify PTCs (e.g., Nelson et al. 2008); comparisons between these methods will be made in a future study. We also used a monopolar probe and pTP masker, resulting in a lower degree of current focusing compared to another study that found a strong correlation between highly focused

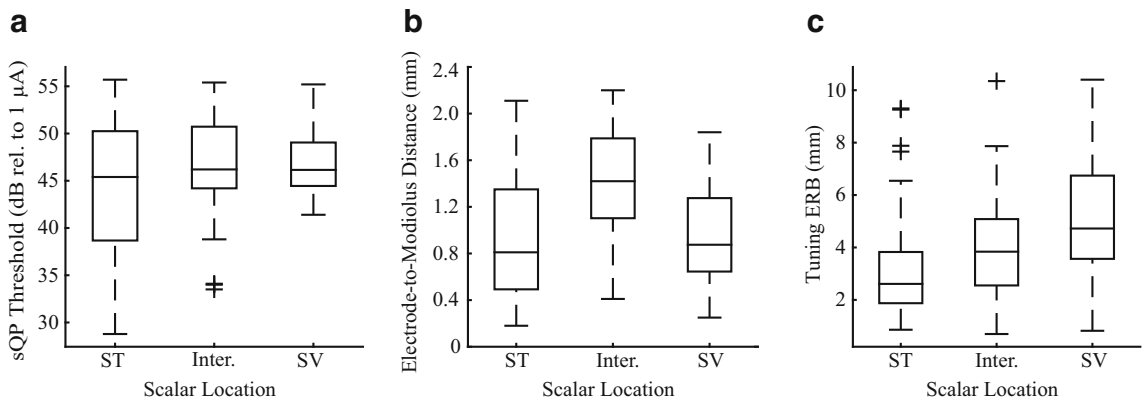

FIG. 6. Box-and-whisker plots for the distribution of scalar location relative to **a** sQP threshold (dB rel. to 1 μA), **b** electrode position (mm), and **c** PTC ERB_{DR} (mm). Scalar location is labeled as scala tympani (ST), intermediate, and scala vestibuli (SV)

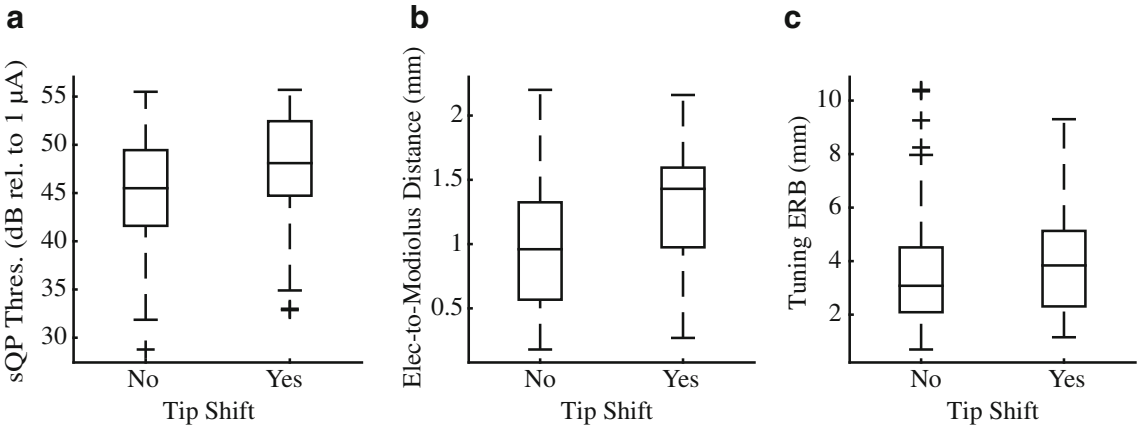

FIG. 7. Box-and-whisker plots for the distribution of PTC tip shifts relative to **a** sQP threshold (dB rel. to 1 μA), **b** electrode position (mm), and **c** PTC ERB_{DR} (mm). Tip shifts are coded either absent ("no") or present ("yes") or for all 182 PTCs in this data set

PTCs and behavioral thresholds (Bierer and Faulkner 2010). Finally, the use of %DR to set probe levels does not guarantee that the probes were equally loud for the listener, though PTC widths have been shown to be insensitive to probe level (Nelson et al. 2008, 2011). It may be this methodological "noise" in the PTC measure weakened the correlations between PTC ERB_{DR}s, sQP thresholds, and electrode-to-modiolus distance for some subjects.

Effects of Scalar Location

Electrodes translocated from ST to SV had higher sQP thresholds, greater electrode-to-modiolus distances, and broader PTC ERB_{DR}s (Fig. 6), consistent with a recent study (DeVries et al. 2016). These results are reflective of the physical distance between electrodes located in ST and those in SV (Teymouri et al. 2011), which likely leads to increased current requirements and broader spread of excitation.

Shepherd et al. (1993) evaluated EABR thresholds in implanted adult cats at different scalar locations within ST. EABR thresholds were reduced when moving from lateral electrode placements to peripheral dendrite and spiral ganglion cell body positions. Frijns et al. (1995, 1996) extended this work using a computational model examining the same ST positions as the Shepherd study, with comparable results. These findings have also been observed in a guinea pig model (Snyder et al. 2004).

Some studies have found that a greater number of electrodes located in SV correlates with poorer CNC word recognition (Finley et al. 2008; Holden et al. 2013); however, we were unable to replicate that finding with these data. ($T_{12} = 1.07$, $P = .31$).

These results support the contention that ST is the ideal scalar location for electrode array insertion, although behavioral and electrophysiological variability is noted even within ST. Given previously observed relationships between scalar location and word recognition (Holden et al. 2013), this underlines the importance of surgical technique and electrode array design to optimize implant insertions.

PTC Tip Shifts and Electrode-to-Modiolus Distances

There were 39 tip shifts out of a possible 182 PTCs, with no evidence of a predominance of apical or basalward shifts, as seen by others (Nelson et al. 2008). PTC tip shifts were analyzed across subjects and electrodes in relation to sQP threshold, electrode-to-modiolus distance, and PTC ERB_{DR} (Fig. 7).

There was no significant relationship between PTC tip shifts and sQP threshold or PTC ERB_{DR}s. This is inconsistent with other studies that have found electrodes with tip shifts tend to have broader PTCs (Nelson et al. 2008; Bierer and Faulkner 2010). It is possible we did not replicate this result due to the very small number of tip shifts larger than one electrode contact observed in this study; it may be that more dramatic tip shifts are needed to observe these relationships.

Electrodes farther from the modiolus tended to have more tip shifts; this is perhaps unexpected, as tip shifts are traditionally viewed as indicative of neural status. Bierer et al. (2010) measured forward-masked PTCs in the inferior colliculus of guinea pigs, and found PTC tips shifted toward the apex where the guinea pig cochlea tapers, causing the apical electrodes to be much closer to the modiolus. In the present study, it is possible that asymmetrical current spread occurred for electrodes farther from the modiolus, due to the increase in current required to reach auditory neurons. This spread may have caused a small shift in the tip of the PTC, which was the predominant type of tip shift observed in this data set.

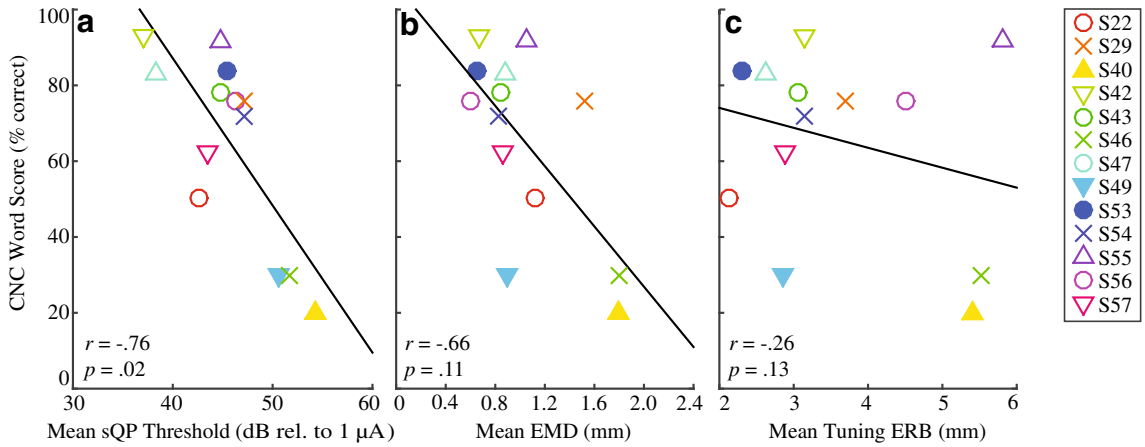

FIG. 8. Correlations between the variables of interest and clinical CNC word scores (% correct). **a** Mean sQP threshold (dB rel. to 1 μA). **b** Electrode-to-modiolus distance (mm). **c** Mean PTC ERB_{DR} (mm). The pre−/peri-lingually deafened subjects (S40, S49, and S53) are represented by filled in symbols, for ease of viewing

Word Recognition

We observed a significant, negative correlation between mean sQP threshold and CNC word recognition in these subjects (Fig. 8a), but no correlation with mean electrode-to-modiolus distance (Fig. 8b) or mean PTC ERB_{DR} (Fig. 8c).

Poorer word recognition in subjects with higher mean focused thresholds is consistent with a recent study in our laboratory (DeVries et al. 2016). However, this result has not been observed by others using bipolar (Pfingst et al. 2004) and phased array stimulation (Long et al. 2014). In the Long study, high within-subject variance for focused thresholds was negatively correlated with the logit-transformed CNC word scores, similar to the findings of Pfingst et al. 2004. We were unable to replicate these results using the within-subject variance of sQP thresholds and raw ($T_{12} = .70$, $P = .50$) and logit-transformed ($T_{12} = .55$, $P = .59$) CNC scores. Long also found that higher RMS error from the threshold-distance correlation was predictive of poorer logit-transformed CNC word recognition scores; subjects with thresholds well predicted by electrode-to-modiolus distance tended to perform better with their implant. The present study did not replicate these results for either raw ($T_{12} = .13$, $P = .90$) or logit-transformed ($T_{12} = -.07$, $P = .95$) CNC word scores, similar to a recent study in our laboratory (DeVries et al. 2016).

Bierer (2007) used the standard deviation of the absolute value of the difference between focused thresholds of adjacent channels, finding a relationship between higher threshold variability and lower CNC word scores. Pfingst et al. (2004) found the same result using the mean of the difference between thresholds. We were unable to replicate the results using the unsigned difference of the standard deviation ($T_{12} = .86$, $P = .41$) or the mean of the difference between thresholds ($T_{12} = -1.34$, $P = .21$).

Zhou et al. (2018) found that steeper multipulse integration (MPI) functions measured with bipolar stimulation were correlated with lower speech reception thresholds. MPI measures have been shown to predict spiral ganglion neural density in implanted guinea pigs (Zhou et al. 2015), thus pointing to a possible relationship between behavioral threshold-related measurements and neural survival.

Given that the present study was unable to replicate results from some of the above studies, it is likely due to a limitation within this dataset, possibly due to insufficient variability in CNC word scores.

The finding that there is no relationship between mean electrode-to-modiolus distance and word recognition is consistent with recent studies (Long et al. 2014; Holden et al. 2013; van der Marel et al. 2015; DeVries et al. 2016), though Aschendorff et al. (2007) did observe that perimodiolar insertions tended to result in better speech outcomes. van der Marel et al. (2015) examined six electrode position-related factors and did not find any correlations with word recognition, but did find that duration of deafness and preoperative word scores correlated with speech outcomes, as others have found (Blamey et al. 2013).

There was no correlation between PTC ERB_{DR} and word recognition, consistent with other studies (Cohen et al. 2003; Anderson et al. 2011; Nelson et al. 2011), though the Anderson study did find a positive correlation between the inverse of the PTC bandwidth and sentence recognition. This is also consistent with previous studies that used the ECAP (Brown et al. 1990; Cohen et al. 2003; Hughes and Abbas 2006), and one that measured ECAP ERB_{DR}s

in all available electrodes (DeVries et al. 2016). Constraints introduced by the speech processor may make it difficult to compare spatial spread measured via direct stimulation to speech recognition, as suggested by others (Nelson et al. 2008, 2011; Anderson et al. 2011).

Duration of deafness was negatively correlated with CNC word scores ($T_{12} = -2.68$, $P = .02$). It is possible that pooling the pre/peri- and post-lingually deafened subjects weakened the correlations between the variables of interest and CNC word scores. However, one pre-lingually deafened subject (S53) scored 84 % on CNC words, and a post-lingually deafened subject (S46) is a much poorer performer (Fig. 8). Central mechanisms and plasticity resulting from deprivation during auditory development are not well understood in humans. It has been suggested that variability in central plasticity may contribute to a variability in performance into adulthood (Lazard et al. 2012).

While PTC ERB_{DR}s were correlated with electrode-to-modiolus distance, they were not correlated with word recognition. The fact that position-related factors did not correlate with word recognition, but duration of deafness and mean focused thresholds did, suggests that additional factors at the ENI are stronger contributors to word recognition.

CONCLUSIONS

The widely documented variability in CI listener outcomes is likely due, in part, to the status of the electrode-neuron interface. Quantifying and disambiguating factors that contribute to poor electrode-neuron interfaces that may be useful for optimization of programming techniques for these listeners. The ability to evaluate the electrode-neuron interface in the clinical environment is limited due to resources, time, and costs. Therefore, identifying measurements that may help to bypass these limitations is of the utmost importance.

This study demonstrated that a measure of spatial spread of excitation, or channel interaction, was correlated with electrode-to-modiolus distance, but not with behavioral thresholds. Scalar location appears to influence behavioral thresholds, degree of channel interaction, and electrode-to-modiolus distance, indicating that proper placement of the electrode array may have an influence on psychophysical and objective measurements.

Behavioral thresholds were the only variable correlated with word recognition. This may indicate that while spatial measures of channel interaction reflect an important aspect of the electrode-neuron interface, and may prove useful for device programming, performance with the implant is not fully captured by electrode position or degree of channel interaction.

Finally, these results suggest that electrode array placement influences spatial spread of excitation and that PTCs may be a useful behavioral measure to disambiguate electrode-neuron interface factors for some CI listeners. Future studies will use PTCs and electrode position to create experimental programs that account for electrodes with high degrees of channel interaction and determine if performance can be meaningfully improved when incorporating this information.

ACKNOWLEDGEMENTS

The authors would like to acknowledge Kelly Jahn for assisting with data collection, Timothy Holden for analyzing the CT scans, and our subjects for their time and dedication.

FUNDING INFORMATION

This study received funding from RO1 DC012142 (JGA) and T32 DC 000033 (University of Washington Speech and Hearing Sciences: LAD).

COMPLIANCE WITH ETHICAL STANDARDS

Conflict of Interest The authors declare that they have no conflict of interest.

REFERENCES

Abbas PJ, Hughes ML, Brown CJ et al (2004) Channel interaction in cochlear implant users evaluated using the electrically evoked compound action potential. Audiol Neurotol 9:203–213

Anderson ES, Nelson DA, Kreft H et al (2011) Comparing spatial tuning curves, spectral ripple resolution, and speech perception in cochlear implant users. J Acoust Soc Am 130:364–375

Aschendorff A, Kromeier J, Klenzner T, Laszig R (2007) Quality control after insertion of the nucleus contour and contour advance electrode in adults. Ear Hear 28:75S–79S

Baayen RH, Davidson DJ, Bates DM (2008) Mixed-effects modeling with crossed random effects for subjects and items. J Mem Lang 59:390–412

Bierer J (2010) Probing the electrode-neuron Interface with focused Cochlear implant stimulation. Trends in Amplif 14:84–95

Bierer JA (2007) Threshold and channel interaction in cochlear implant users: evaluation of the tripolar electrode configuration. J Acoust Soc Am 121:1642–1653

Bierer JA, Bierer SM, Kreft HA, Oxenham AJ (2015) A fast method for measuring psychophysical thresholds across the cochlear implant Array. Trends Hear 19:1–12

Bierer JA, Bierer SM, Middlebrooks JC (2010) Partial tripolar cochlear implant stimulation: spread of excitation and forward masking in the inferior colliculus. Hear Res 270:134–142

Bierer JA, Faulkner KF (2010) Identifying cochlear implant channels with poor electrode-neuron interface: partial tripolar, single-channel thresholds and psychophysical tuning curves. Ear Hear 31:247

Blamey P, Artieres F, Baskent D et al (2013) Factors affecting auditory performance of postlinguistically deaf adults using cochlear implants: an update with 2251 patients. Audiol Neurotol 18:36–47

Briaire JJ, Frijns JHM (2006) The consequences of neural degeneration regarding optimal cochlear implant position in scala tympani: a model approach. Hear Res 214:17–27

Brown CJ, Abbas PJ, Gantz B (1990) Electrically evoked whole-nerve action potentials: data from human cochlear implant users. J Acoust Soc Am 88:1385–1391

Cohen LT (2009) Practical model description of peripheral neural excitation in cochlear implant recipients: 2. Spread of the effective stimulation field (ESF), from ECAP and FEA. Hear Res 247:100–111

Cohen LT, Richardson LM, Saunders E, Cowan RS (2003) Spatial spread of neural excitation in cochlear implant recipients: comparison of improved ECAP method and psychophysical forward masking. Hear Res 179:72–87

Cohen LT, Saunders E, Clark GM (2001) Psychophysics of a prototype peri-modiolar cochlear implant electrode array. Hear Res 155:63–81

DeVries L, Scheperle R, Bierer JA (2016) Assessing the electrode-neuron interface with the electrically evoked compound action potential, electrode position, and behavioral thresholds. J Assoc Res Otolaryngol 17:237–252

Finley CC, Holden TA, Holden LK et al (2008) Role of electrode placement as a contributor to variability in cochlear implant outcomes. Otol Neurotol 29:920–928

Frijns JH, de Snoo SL, Schoonhoven R (1995) Potential distributions and neural excitation patterns in a rotationally symmetric model of the electrically stimulated cochlea. Hear Res 87:170–186

Frijns JH, de Snoo SL, ten Kate JH (1996) Spatial selectivity in a rotationally symmetric model of the electrically stimulated cochlea. Hear Res 95:33–48

Goldwyn JH, Bierer SM, Bierer JA (2010) Modeling the electrode-neuron interface of cochlear implants: effects of neural survival, electrode placement. and the partial tripolar configuration Hear Res 268:93–104

Hall RD (1990) Estimation of surviving spiral ganglion cells in the deaf rat using the electrically evoked auditory brainstem response. Hear Res 49:155–168

Hinojosa R, Lindsay JR (1980) Profound deafness. Associated sensory and neural degeneration. Arch Otolaryngol 106:193–209

Holden LK, Finley CC, Firszt JB et al (2013) Factors affecting open-set word recognition in adults with cochlear implants. Ear Hear 34:342–360

Hughes ML, Abbas PJ (2006) Electrophysiologic channel interaction, electrode pitch ranking, and behavioral threshold in straight versus perimodiolar cochlear implant electrode arrays. J Acoust Soc Am 119:1538–1547

Hughes ML, Stille LJ (2008) Psychophysical versus physiological spatial forward masking and the relation to speech perception in cochlear implants. Ear Hear 29:435–452

Jones GL, Ho Won J, Drennan WR, Rubinstein JT (2013) Relationship between channel interaction and spectral-ripple discrimination in cochlear implant users a. J Acoust Soc Am 133:425–433

Kalkman RK, Briaire JJ, Dekker DMT, Frijns JHM (2014) Place pitch versus electrode location in a realistic computational model of the implanted human cochlea. Hear Res 315:10–24

Kawano A, Seldon HL, Clar GM (1998) Intracochlear factors contributing to psychophysical percepts following cochlear implantation. Acta Otolaryngol 118:313–326

Khan AM, Handzel O, Damian D et al (2005) Effect of cochlear implantation on residual spiral ganglion cell count as determined by comparison with the contralateral nonimplanted inner ear in humans. Ann Otol Rhinol Laryngol 114:381–385

Koch DB, Osberger MJ, Segel P, Kessler D (2004) HiResolution™ and conventional sound processing in the HiResolution™ bionic ear: using appropriate outcome measures to assess speech recognition ability. Audiol Neurotol 9:214–223

Landsberger DM, Srinivasan AG (2009) Virtual channel discrimination is improved by current focusing in cochlear implant recipients. Hear Res 254:34–41

Lazard DS, Giraud A-L, Gnansia D et al (2012) Understanding the deafened brain: implications for cochlear implant rehabilitation. Eur Ann Otorhinolary 129:98–103

Linthicum FH, Fayad J, Otto SR et al (1991) Cochlear implant histopathology. Am J Otol 12:245–311

Litvak LM, Spahr AJ, Emadi G (2007) Loudness growth observed under partially tripolar stimulation: model and data from cochlear implant listeners. J Acoust Soc Am 122:967–981

Long CJ, Holden TA, McClelland GH et al (2014) Examining the electro-neural interface of cochlear implant users using psychophysics, CT scans, and speech understanding. J Assoc Res Otolaryngol 15:293–304

McKay CM (2012) Forward masking as a method of measuring place specificity of neural excitation in cochlear implants: a review of methods and interpretation. J Acoust Soc Am 131:2209–2224

Nelson DA, Donaldson GS, Kreft H (2008) Forward-masked spatial tuning curves in cochlear implant users. J Acoust Soc Am 123:1522–1543

Nelson DA, Kreft HA, Anderson ES, Donaldson GS (2011) Spatial tuning curves from apical, middle, and basal electrodes in cochlear implant users. J Acoust Soc Am 129:3916–3933

Pfingst BE, Bowling SA, Colesa DJ et al (2011) Cochlear infrastructure for electrical hearing. Hear Res 281:65–73

Pfingst BE, Xu L, Thompson CS (2004) Across-site threshold variation in cochlear implants: relation to speech recognition. Audiol Neurotol 9:341–352

Ramekers D, Versnel H, Strahl SB et al (2014) Auditory-nerve responses to varied inter-phase gap and phase duration of the electric pulse stimulus as predictors for neuronal degeneration. J Assoc Res Otolaryngol 15:187–202

Sęk A, Alcántara J, Moore BCJ et al (2005) Development of a fast method for determining psychophysical tuning curves. Int J Audiol 44:408–420

Shepherd RK, Hatsushika S, Clark GM (1993) Electrical stimulation of the auditory nerve: the effect of electrode position on neural excitation. Hear Res 66:108–120

Shepherd RK, Javel E (1997) Electrical stimulation of the auditory nerve. I. Correlation of physiological responses with cochlear status. Hear Res 108:112–144

Skinner MW, Ketten DR, Holden LK et al (2002) CT-derived estimation of cochlear morphology and electrode array position in relation to word recognition in nucleus-22 recipients. J Assoc Res Otolaryngol 3:332–350

Smith L, Simmons FB (1983) Estimating eighth nerve survival by electrical stimulation. Ann Otol Rhinol Laryngol 92:19–23

Snyder RL, Bierer JA, Middlebrooks JC (2004) Topographic spread of inferior colliculus activation in response to acoustic and intracochlear electric stimulation. J Assoc Res Otolaryngol 5:305–322

Srinivasan AG, Landsberger DM, Shannon RV (2010) Current focusing sharpens local peaks of excitation in cochlear implant stimulation. Hear Res 270:89–100

Teymouri J, Hullar TE, Holden TA, Chole RA (2011) Verification of computed tomographic estimates of cochlear implant array position: a micro-CT and histologic analysis. Otol Neurotol 32:980–986

van der Marel KS, Briaire JJ, Verbdrist BM et al (2015) The influence of cochlear implant electrode position on performance. Audiol Neurotol 20:202–211

Verbist BM, Frijns JH, Geleijns J, Van Buchem MA (2005) Multisection CT as a valuable tool in the postoperative assessment of cochlear implant patients. Am J of Neuroradiol 26:424–429

Won JH, Drennan WR, Rubinstein JT (2007) Spectral-ripple resolution correlates with speech reception in noise in cochlear implant users. J Assoc Res Otolaryngol 8:384–392

Zhou N, Dong L, Hang M (2018) Evaluating multipulse integration as a neural-health correlate in human cochlear implant users: effects of stimulation mode. J Assoc Res Otolaryngol 19:99–111

Zhou N, Kraft CT, Colesa DJ, Pfingst BE (2015) Integration of pulse trains in humans and guinea pigs with cochlear implants. J Assoc Res Otolaryngol 16:523–534

Zhou N, Pfingst BE (2016) Evaluating multipulse integration as a neural-health correlate in human cochlear-implant users: relationship to spatial selectivity. J Acoust Soc Am 140:1537–1547